Proceedings of the ASME 2010 3rd Joint US-European Fluids Engineering Summer Meeting and 8th International Conference on Nanochannels, Microchannels, and Minichannels
FEDSM-ICNMM2010
August 1-5, 2010, Montreal, Canada

FEDSM-ICNMM2010-31127

FUZZY CLUSTERING OF VERTICAL TWO PHASE FLOW REGIMES BASED ON IMAGE PROCESSING TECHNIQUE

Soheil Ghanbarzadeh
M.Sc. Student
School of Mechanical Engineering
Sharif University of Technology
Tehran, Iran

Pedram Hanafizadeh
PhD Candidate
School of Mechanical Engineering
Sharif University of Technology
Tehran, Iran

Mohammad Hassan Saidi
Professor and chairman
School of Mechanical Engineering
Sharif University of Technology
Tehran, Iran

Ramin Bozorgmehry B.
Associate Professor
School of Chemical and Petroleum Engineering
Sharif University of Technology
Tehran, Iran

ABSTRACT

In order to safe design and optimize performance of industrial systems which work under two phase flow conditions, it's often needed to categorize flow into different regimes. In present work the experiments of two phase flow were done in a large scale test facility with length of 6m and 5cm diameter. Four main flow regimes were observed in vertical air-water two phase flows at moderate superficial velocities of gas and water: Bubbly, Slug, Churn and Annular. Some image processing techniques were used to extract information from each picture. This information include number of bubbles or objects, area, perimeter, height and width of objects (second phase).Also a texture feature extraction procedure was applied to images of different regimes. Some features which were adequate for regime identification were extracted such as Contrast, Energy, Entropy and etc. To identify flow regimes a fuzzy interface was introduced using characteristic of second phase in picture. Also an Adaptive Neuro Fuzzy (ANFIS) was used to identify flow patterns using textural features of images. The experimental results show that these methods can accurately identify the flow patterns in a vertical pipe.

INTRODUCTION

Gas/liquid multiphase flows occur in a wide range of natural and man-made situations. Examples include boiling heat transfer, cloud cavitations, bubble columns and reactors in the chemical industry, cooling circuits of power plants, spraying of liquid fuel and paint. Two-phase gas-liquid pipe flow is a complex phenomenon which involves interactions between the phases such as interfacial transfer (mass, momentum and energy), entrainment or flooding. As a result of these interactions, two-phase flow can appear in different forms that are very important to identify in order to determine the properties of the system.

Vertical two-phase flows are usually classified into four basic flow regimes [1-3]. A gradual increment in the gas flow rate consecutively produces the bubbly, slug, churn and annular flow patterns when an upward liquid flow in a vertical pipe with a constant liquid flow rate is considered (Fig.1). The main difference between slug and churn flow can be investigated as the turbulence and vibrations in churn flow are much higher than the slug flow. Identification of gas-liquid two-phase flow regime may be done by two main ways: one is direct observation such as visual method and high-speed photography, and the other is extraction of characteristic variables from signals of two-phase flow [4]. Pressure and pressure drop signals are acquired easily in most cases thus were widely used as the main signals for flow pattern identification and the fractal method was applied to analyze the signals to identify flow regimes. Void fraction is also used to identify the flow regimes.

Already Corre et al. [5] used complicated features of flow such as local void fraction and local volumetric interfacial area

to classify two phase flows into different regimes. In their work, measurements of local void fraction and interfacial area have been done thanks to a four-sensor conductivity probe. Mi et al. [6] did a similar work that relies on a fuzzy-neural hybrid system processing and interpreting impedance based on measuring the electrical impedance of a given two-phase mixture. In another paper, a new method to identify flow regime in two-phase flow was presented by Zhou et al. [7], based on combined use of image multi-feature fusion and support vector machine. In a recent work by Lilian Shi [8] a fuzzy reasoning method was used to identify stratified flow and annular flow in horizontal tube. Then a fuzzy neural network was used to identify the flow pattern of bubbly, slug and plug. He used a simple image processing technique to obtain the characteristics of bubbles such as area, width and height. Sunde et al. [9] did a precise work which is based on image processing of data obtained partly from dynamic neutron radiography recordings of real two-phase flow in a heated metal channel, and partly by visible light from a two-component mixture of water an air. They performed the classification of the flow regime type by an artificial neural network (ANN) algorithm.

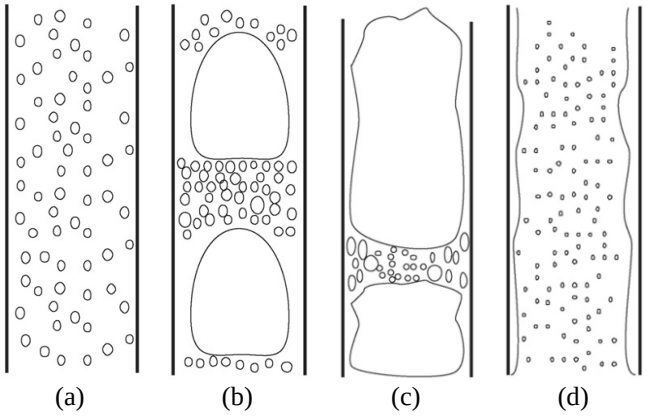

Fig.1. Two phase flow regimes in vertical pipe: a. bubbly, b. slug, c. churn and d. annular.

The first image processing works in two and multiphase flows were presented by Misawa M. [10], Gopaland Jepson [11], Hesieh et al. [12] and T. B. Dinh [13]. Lilian Shi et al. [14] presented a new method to measure flowing parameters in two-phase flow. He used an image-subtracted algorithm to remove the background noise. Also some morphological functions were applied to modify bubbles shape. His method can measure the bubbles area, perimeter, diameter, gas area fraction and bubbles velocity in gas-liquid two-phase bubbly flow. Mayor et al. [15] performed a simple work to provide information concerning a straightforward and accurate image analysis technique, developed specially for the study of continuous gas–liquid slug flow, in vertical columns, and applicable for the measurement of a large number of bubbles. They presented a detailed assessment of the uncertainty associated with the parameters measured by this technique. In a recent research by H. Wang and F. Dong [16] gray level co-occurrence matrix (GLCM) and the gray level-gradient co-occurrence matrix (GLGCM) were applied to analyze the flow texture of the gas/liquid two-phase flow. Experiments were carried out with high-speed camera recording system. Gas/liquid two-phase flow images were processed by digital image processing method. Texture features of the experimental images were extracted and analyzed by GLCM and GLGCM respectively.

In present work flow regime identification was carried out by Fuzzy algorithm and Nero-fuzzy methodology using image processing technique for flow feature extraction and image feature extraction. Flow features were selected as number of air bubbles, area and perimeter of each bubble, mean area and perimeter of air particles and maximum of these quantities. The image texture features were chosen to be the energy, entropy, homogeneity and cluster prominence. The images of regimes were captured by a high speed CCD camera. The results show that combination of image texture analysis (image feature extraction) with ANFIS (Adaptive Neuro Fuzzy Interface System) is more accurate than combination of flow characteristic (flow feature extraction) with fuzzy reasoning.

EXPERIMENTAL SET-UP

The experimental apparatus is shown schematically in Fig. 2. The water flow rates were regulated by two globe valves and were measured by the calibrated magnetic flow meter [Siemens MAG5100] with an accuracy of 0.25%. The compressed air was fed by a compressor [Atlas Copco GA210] up to 6 bar continuously. The air flow rates were set and filtered by the Wilkerson filter and regulator and were measured by the calibrated Gas Turbine flow meter [Omega FTB-934] with an accuracy of ±1%. Air and water are mixed together in the plenum which is made of acrylic glass and placed at the bottom of the riser pipe. Compressed air is injected at the plenum by the porous stainless steel plate with 108 holes of 0.5 mm diameter. The overall length and internal diameter of the riser pipe are 6 m and 50 mm, respectively. In order to have the capability of visual observation of the two phase flow patterns, the riser pipe is made of a transparent acrylic glass. The water flowed upward with air through the riser and would be separated in the separation tank at the top of the riser. The air was discharged to the atmosphere and the water was returned to the main tank or to the airlift tank. The temperature of the water was kept constant at the ambient condition. The pressure of the two phase flow is measured by the 16 pressure transmitters [INDUMART, PTF106-04G100] with accuracy of 0.3% at different position along the riser. All the above instruments own a specified signal (4-20 mA); these signals are scaled and fed for a rapid and wide band data acquisition card of type National Instrument, PCI-6255. Recorded data are stored for further post processing. The flow regimes were observed by a high speed CCD camera [CASIO F1] with 1200 frame per second. Images were captured at the height of 5.5 m with 60 fps and resolution of 6 Mega-pixels (2816×2112). The superficial air and water

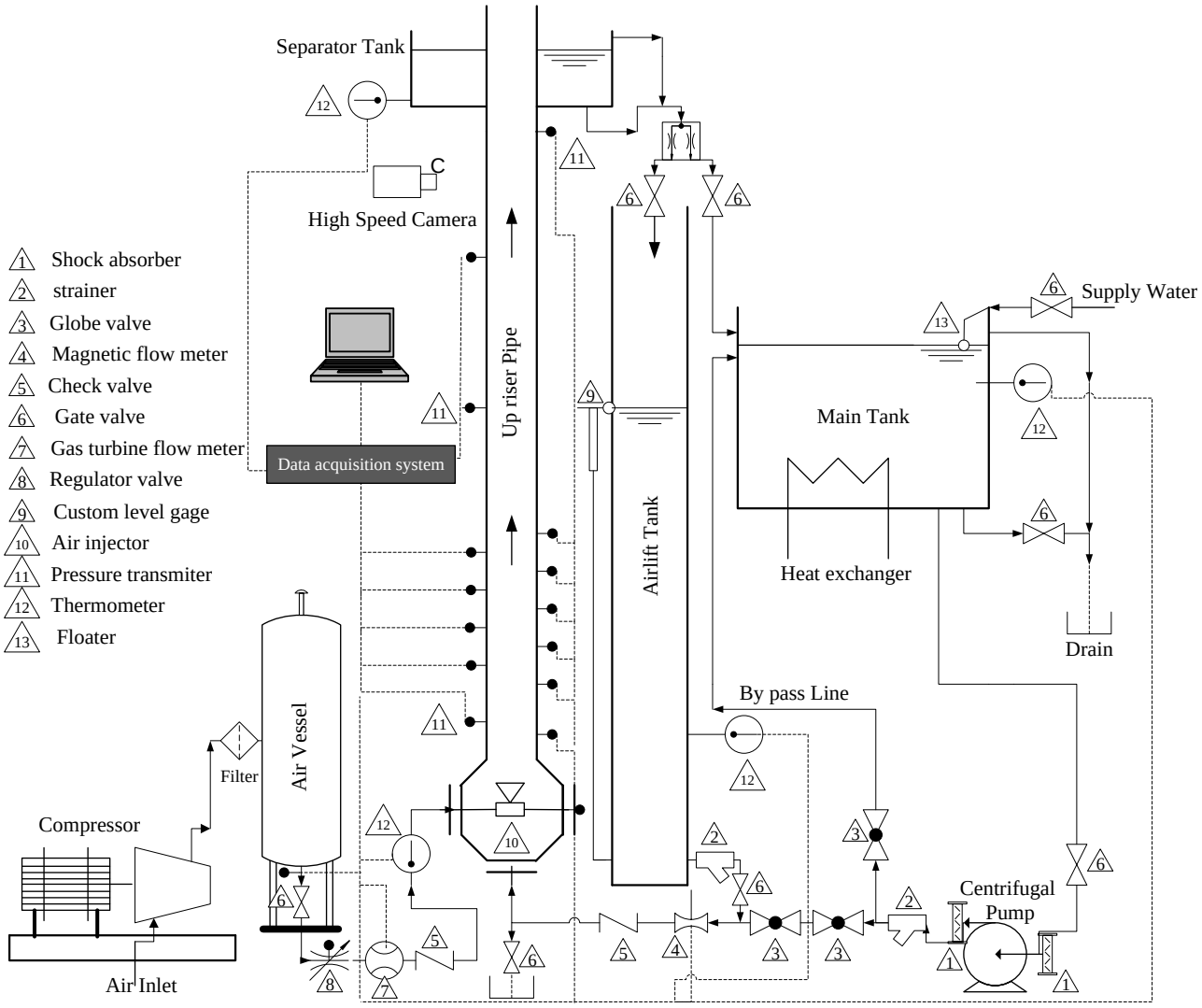

Fig.2. Schematic view for the experimental system

velocity were set to be 0.01-10 m/s and 0.1-5 m/s, respectively.

IMAGE PROCESSING

Flow Feature Extraction

In order to visualize various two phase flow pattern in the up-riser of airlift pump, a set of experiment was done in a two-phase flow field. Flow field was captured with a high speed digital camera (60 frame/second and 1/2000 s shutter speed) and the results were analyzed with a simple image processing scheme.

Some image processing technique must be done in order to extract feature from the images of two-phase flow [17]. Pictures were in 8bits RGB (red, green and blue) color format. They were converted from RGB to grey scale mode. The output images have 256 grey levels, from 0 (black) to 255 (white). It might be difficult to extract the bubbles directly from original digital images, therefore, some preprocessing procedures must be done to reduce noises and improve the quality of the images. An image-subtracted algorithm was used to reduce the background noise by subtracting the background image from the each dynamic image. In order to smooth the image border, a median filter was also used. It is particularly useful to reduce speckle, salt and pepper noises. Its edge-preserving nature makes it useful in cases where edge blurring is undesirable. A sliding window (3×3) was used in this process, and the median gray level of the pixels in the window is calculated, then the gray level of the pixel located at the center of the window was replaced by the median. The results of these processes for bubbly flow are shown in Fig.3.

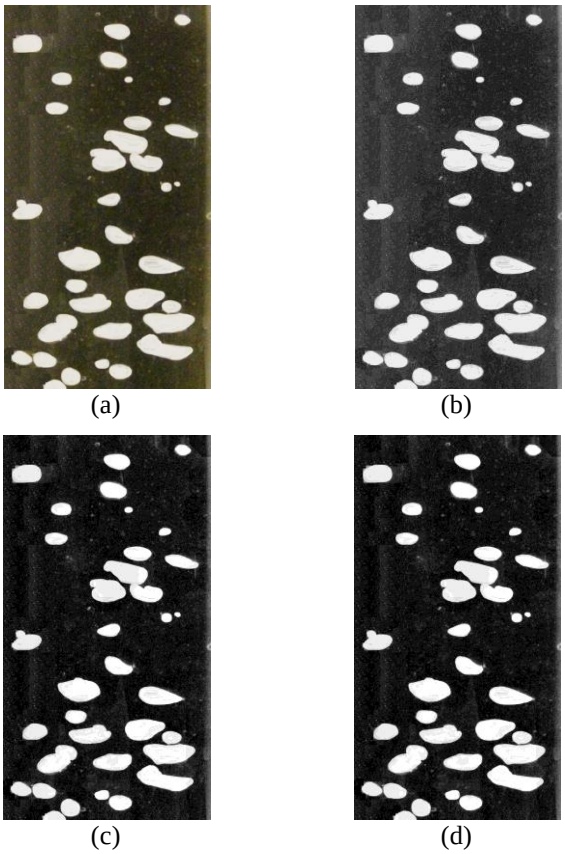

(a) (b) (c) (d)

Fig.3. a. RGB picture, b. gray picture, c. background subtracted and d. median process of bubbly flow image

The images were converted from grayscale to binary mode by threshold segmentation, and an iteration algorithm was used to calculate the optimizing threshold, as follows:

a. Calculate the minimum $Z_1$and maximum Z_K of gray level in the image, and define the initial value of threshold as

$$T^0 = \frac{Z_k + Z_l}{2}$$

b. Segment the image into object and background two parts according to the threshold T^k, and calculate the average value Z_0 and Z_B of the two parts as

$$Z_0 = \sum_{Z(i,j)<T^k} \frac{Z(i,j)}{N_0}$$

$$Z_B = \sum_{Z(i,j)>T^k} \frac{Z(i,j)}{N_B}$$

where, Z(i,j) is the gray level of the pixel (i,j) in the image, $N_0$is the number of the pixels which Z(i,j) is less than T^k, and N_B is the number of the pixels which Z(i,j)is more than T^k.

c. Calculate the new threshold as

$$T^k = \frac{Z_0 + Z_B}{2}$$

if $T^k \cong T^{k+1}$, then end, else $k \Leftarrow k+1$, and turn to step b. The final binary image is shown in Fig.4.

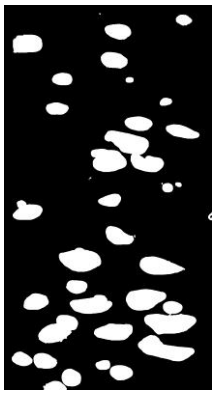

Fig.4. Binary image of bubbly two phase flow

Finally, some morphological functions (such as dilation, erosion opening and closing operation, etc) were applied to modify the shape of bubbles. Dilation adds pixels to the boundaries of objects in an image, while erosion removes pixels on object boundaries. The definition of a morphological opening of an image is erosion followed by dilation, using the same structuring element for both operations. The related operation, morphological closing of an image, is the reverse; it consists of dilation followed by erosion with the same structuring element. Both do not significantly alter the area or shape of objects. Opening operation removes small objects and smoothes boundaries. Borders removed by erosion are restored by dilation, but small objects that were absorbed during erosion do not reappear after dilation. Closing operation was used to fill tiny holes and smoothes boundaries. Objects were expanded by dilation and then reduced by erosion, so borders were smoothed and holes were filled. After all these operations, the results of mentioned image processing techniques are shown in Fig.5.

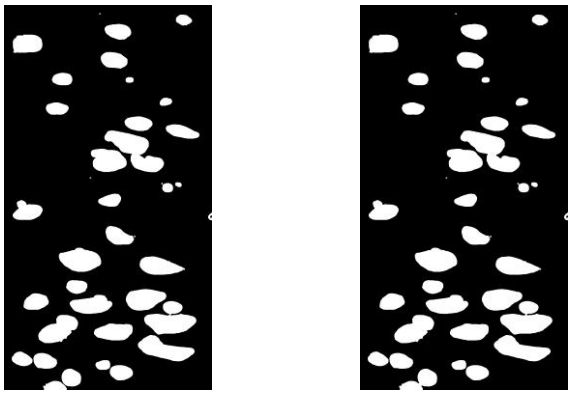

a) Opening b) Closing

Fig.5. Final result of image processing of bubbly two phase flow

Table1. Extracted features of each regime (all units are pixel)

Feature	Bubbly	Slug	Churn	Annular
Number of objects	19-67	4-16	3-6	1
Mean Area	3119-11574	4×10^4-3.2×10^5	1.8×10^5-3.7×10^5	1.1×10^6-2.5×10^6
Area of biggest object	21298-38924	8.9×10^4-8.1×10^5	9.3×10^5-1.9×10^6	1.1×10^6-2.5×10^6
Mean Perimeter	181-392	612-2105	1514-2356	3781-5614
Perimeter of biggest object	517-712	1014-3196	3418-5111	3781-5614
Height of biggest object	59-173	421-1214	1378-1823	2000
Width of biggest object	51-219	842-1002	865-1011	882-1023
PCBIE	0	0.19	0.71	1

In Fig.6 results of same image processing procedure are shown for slug, churn and annular. In these pictures air-water boundary are visible and detectable, and now these images are ready for post processing. By this method some features are able to be extracted automatically and instantaneously; such as number of bubbles or slugs, length of objects, their area and perimeter.

(a) (b) (c)

Fig.6. Final processed picture of a. slug, b. churn and c. annular flow patterns in airlift pump

In order to obtain a clear view of pipe in pictures, original images were cropped from larger images (6 Mega-pixels) to 1100×2000 pixels images. Processing more than 50 images per each regime leads to extracting features such as number of objects, max area and perimeter, mean area and perimeter, width and length of objects and image. The results are summarized in table 1. In this table the variation of selected properties in different images are shown. As we see the extracted features of slug and churn flow are alike. So we have some complexity to distinguish these two regimes. For this reason a simple but accurate analysis must be added to the procedure.

From images of flow regimes it is obvious that second phase (air) in slug flow has a round and smooth boundary. Also its boundary does not usually meet the image boundaries; unless in one edge. Regarding this note if fuzzy system recognizes that the flow regime is slug or churn some additional condition must be checked and this condition is whether second phase boundaries coincide the image edges or not. Achieving this goal the probability of coincidence of one of boundaries with image edges (PCBIE parameter in table.1) was calculated. The results show that in churn flow this probability is higher.

Image Textural Features Extracting

In this section *gray level co-occurrence matrix* GLCM and related formula for feature extraction are described. This method captures the second order statistics of local image features. GLCM captures the second order statistics of gray level values.

Gray level co-occurrence matrix (GLCM) has been employed in extracting texture features and various image processing applications for a long time. Co-occurrence matrixes which describe the gray level spatial dependency in two dimensional images have been presented in [18].

GLCM could reflect image's synthetically gray information about direction, interval, changing extent and so on. As to a M×N digital image, GLCM is constructed to record the joint probability $p(i,j)$ with two respective neighboring pixels in the image, one with gray level *i* belonging to direction θ and the other with gray level *j* in distance *d*. Usually, θ is set to 0º, 45º, 90º, 135º and *d* is set to 1. The definition of the co-occurrence matrix is shown in the following equation

$$P(i,j,d,\theta) = \{[(x,y),(x+\Delta x, y+\Delta y)]|\, f(x,y) = i, f(x+\Delta x, y+\Delta y) = j; x = 1,2,\dots M; y = 1,2,\dots N\}$$

Where$i,j = 0,1,,\dots L-1$; *x, y* is the coordinate of pixel; *L* is the gray level which is equal to 256 in this research. As above vectors have difference meanings and range, it is necessary to do the inner normalization before storing into the database. For simplicity, direction θ and distance *d* are elided in GLCM expression in this paper. As a character is a token for image texture analysis, GLCM is not applied directly, but calculates the second-order statistics based on the GLCM.

Haralick [19] proposed 14 statistical features which were extracted from the GLCM. Six items from them are chosen and shown in table 2.

Table2. Textural features by GLCM

Texture feature	Calculating Formula
Contrast (f_1)	$f_1 = -\sum_{i=0}^{L-1}\sum_{j=0}^{L-1}\lvert i-j\rvert^2 P_{ij}$
Entropy (f_2)	$f_2 = -\sum_{i=0}^{L-1}\sum_{j=0}^{L-1} P_{ij} \times log_2(P_{ij})$
Energy (f_3)	$f_3 = -\sum_{i=0}^{L-1}\sum_{j=0}^{L-1} P_{ij}^2$
Homogeneity (f_4)	$f_4 = -\sum_{i=0}^{L-1}\sum_{j=0}^{L-1}\frac{P_{ij}}{1+\lvert i-j\rvert^2}$
Correlation (f_5)	$f_5 = \frac{1}{\sigma_x\sigma_y}\sum_{i=0}^{L-1}\sum_{j=0}^{L-1}(i.j)P_{ij} - \mu_x\mu_y$ $\mu_x = \sum_{i=0}^{L-1} i\sum_{j=0}^{L-1} P_{ij}, \mu_y = \sum_{i=0}^{L-1} j\sum_{j=0}^{L-1} P_{ij},$ $\sigma_x^2 = \sum_{i=0}^{L-1}(i-\mu_x)^2\sum_{j=0}^{L-1} P_{ij},$ $\sigma_y^2 = \sum_{i=0}^{L-1}(j-\mu_y)^2\sum_{j=0}^{L-1} P_{ij}$
Cluster prominence (f_6)	$f_6 = \sum_{i=0}^{L-1}\sum_{j=0}^{L-1}[(i-\mu_x) + (j-\mu_y)]^4 P_{ij}$

In this regard a simple code was developed to calculate introduced features. 60 images of each regime which were captured in one second (1000 ms) were used to calculate these parameters. These trends were repeatable during experiments so we neglect to investigate more cases.

Contrast is the difference between the highest and the lowest values of a contiguous set of pixels which indicate the variance of gray levels of the image. The GLCM contrast tends to be highly correlated with spatial frequencies while the module of the displacement vector tends to be one. The low contrast image certainly features low spatial frequencies. Fig.7 shows the variation of contrast versus time. It's obvious that contrast of bubbly flow is the highest and the slug's is the lowest.

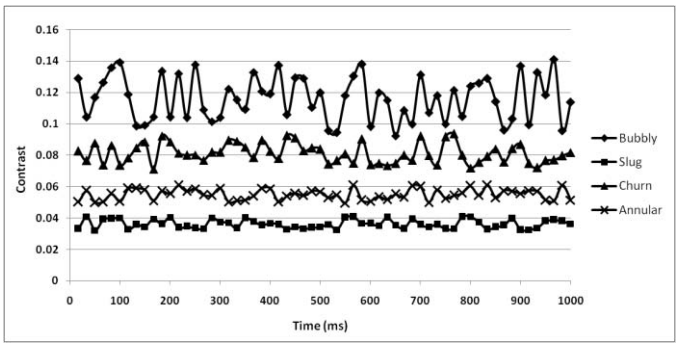

Fig.7. Contrast of images for 4 main regimes

Entropy measures the disorder of an image. When the image is not texturally uniform, many GLCM elements have very small values, which imply that entropy is very large. Fig.8 demonstrates variation of entropy versus time. As it is seen, the entropy of annular flow remains constant while the bubbly has the most variation.

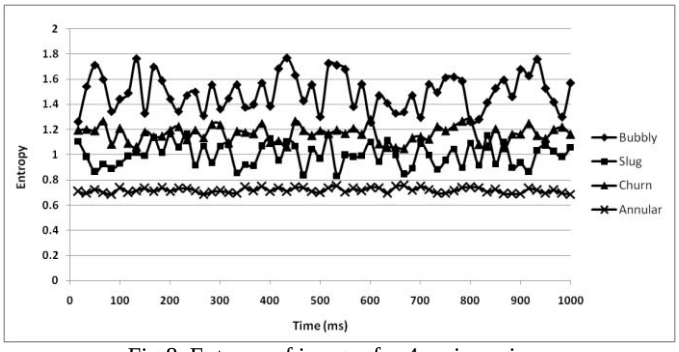

Fig.8. Entropy of images for 4 main regimes

Energy is also called Angular Second Moment. Energy measures textural uniformity, i.e. pixel pairs repetitions. High energy value occurs when the gray level distribution over the window has either a constant or a periodic form. Figure 9 illustrate that the images of bubbly flow have the lowest energy but annular flow has the highest value. For the images of churn and slug flow this quantity is close.

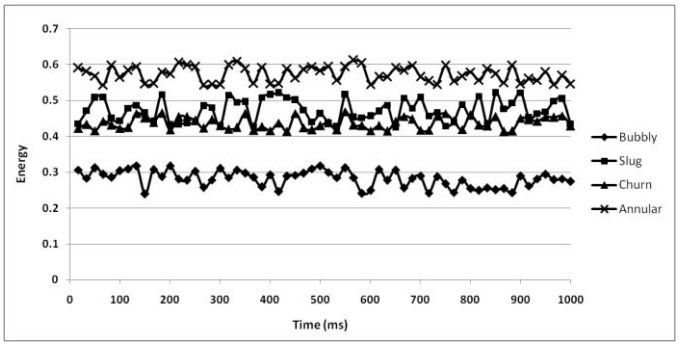

Fig.9. Energy of images for 4 main regimes

Homogeneity is also called inverse difference moment. This parameter measures image homogeneity as it assumes

larger values for smaller gray value differences in pair elements. Homogeneity decreases if contrast increases while energy is kept constant. On the other hand, it decreases if energy increases while contrast is kept constant. After processing 60 images of each regime, as it is shown in Fig.10, the homogeneity of bubbly flow images have the highest value but it takes the lowest value for churn flow images.

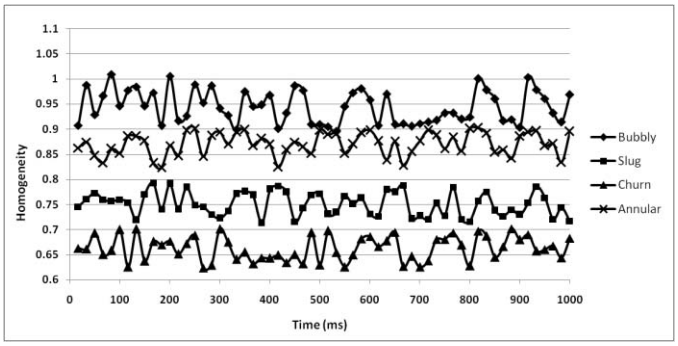

Fig.10. Homogeneity of images for 4 main regimes

Correlation is a measurement of gray tone linear-dependencies in the image; in particular, the direction under investigation is the same as vector displacement. High correlation values imply a linear relationship between the gray levels of pixel pairs. It is obvious from Fig this parameter does not differ for different regimes and it has no regular distribution for different regimes so it is ignored for further post processing.

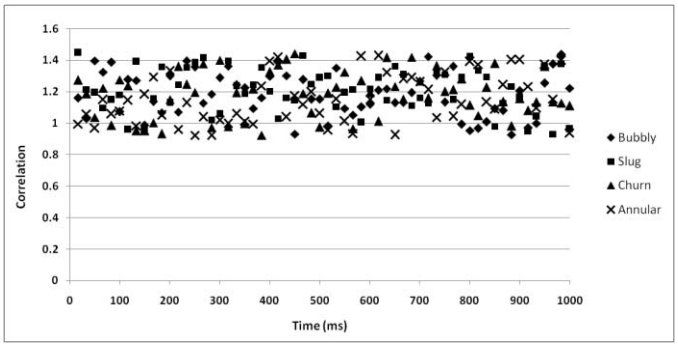

Fig.11. Correlation of images for 4 main regimes

Fig. 12 shows variation of cluster prominence versus times for bubbly, slug, churn and annular regimes. It is clear that this parameter in churn flow is higher in order of magnitude. For bubbly flow the cluster prominence takes the lowest quantity and it increases to slug and then annular.

The obtained results from flow feature extraction (Table1) were used to set up a fuzzy reasoning system which could anticipate regimes based on inlet information of flow images. In addition of this, the investigated textural features of images were applied to train an ANFIS (Adaptive Neuro Fuzzy Interface System) which its detail are presented in next part.

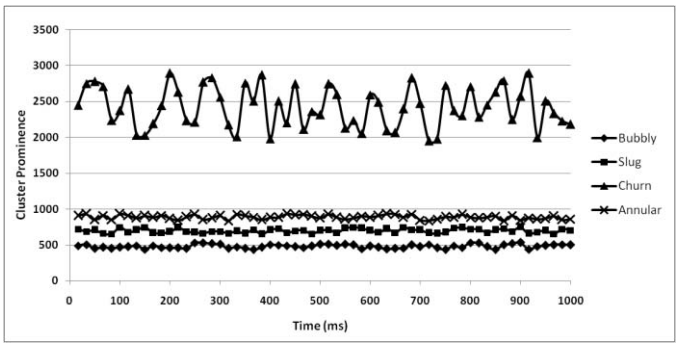

Fig.12. Cluster prominence of images for 4 main regimes

MODELING APPROACH

Fuzzy System

In recent years, the number and variety of applications of fuzzy logic have increased significantly. The applications range from consumer products such as cameras, camcorders, washing machines, and microwave ovens to industrial process control, medical instrumentation, decision-support systems, and portfolio selection.

Fuzzy logic has two different meanings. In a narrow sense, fuzzy logic is a logical system, which is an extension of multivalve logic. However, in a wider sense fuzzy logic is almost synonymous with the theory of fuzzy sets, a theory which relates to classes of objects with unsharp boundaries in which membership is a matter of degree. Even in its more narrow definition, fuzzy logic differs both in concept and substance from traditional multivalve logical systems.

One of the most important and basic concept underlying fuzzy logic (FL) is linguistic variable, that is, a variable whose values are words rather than numbers. In effect, much of FL may be viewed as a methodology for computing with words rather than numbers. Although words are inherently less precise than numbers, their use is closer to human intuition. Furthermore, computing with words exploits the tolerance for imprecision and thereby lowers the cost of solution.

Another basic concept in FL, which plays a central role in most of its applications, is that of a fuzzy if-then rule or, simply, fuzzy rule. Although rule-based systems have a long history of use in Artificial Intelligence (AI), what is missing in such systems is a mechanism for dealing with fuzzy consequents and fuzzy antecedents. In fuzzy logic, this mechanism is provided by the calculus of fuzzy rules. The calculus of fuzzy rules serves as a basis for what might be called the Fuzzy Dependency and Command Language (FDCL). In most of the applications of fuzzy logic, a fuzzy logic solution is, in reality, a translation of a human solution into FDCL.

As we used fuzzy logic to divide the flow pattern (our universe of discourse) to 4 main regimes there is no definite boundary between two patterns .In the other words the universe of discourse which is shown in Fig.13 force us to change gradually from one pattern to another. An additional note that must be considered here is patterns can be divided to 6 regimes:

single phase liquid, bubbly, slug, and churn and annular and single phase gas. Corre et al. [5] considered the first 4 regimes in their work, i.e. they ignored annular and single phase gas.

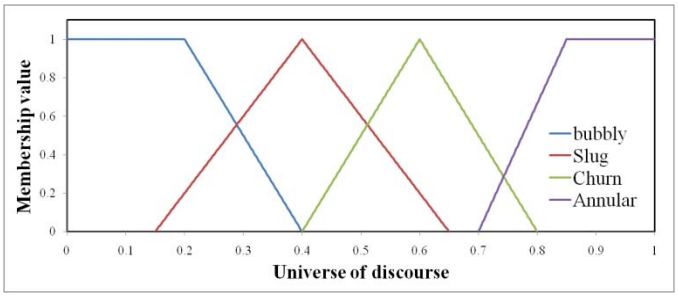

Fig.13. Membership for our fuzzy system outputs

Figure 13 shows the universe of discourse in which our flows were divided to 4 two phase regimes. The distribution of regimes was carried out such that the contribution of slug with bubbly and churn are large areas. The bubbly flow occupies the most area and annular has the lowest. This distribution has been obtained with large amount of try and again procedure.

The four selected fuzzy inputs are the number of objects in image, area of biggest object, mean perimeter of objects and PCBIE. Different choices for each of these fuzzy variables are allowed. For each input the fuzzified parameters are shown in Fig.14. This membership functions were found to be effective and more reliable in order to have accurate result. In other words after testing a large number of flow features which were extracted from images this functions were used as our membership function to classify flow regimes.

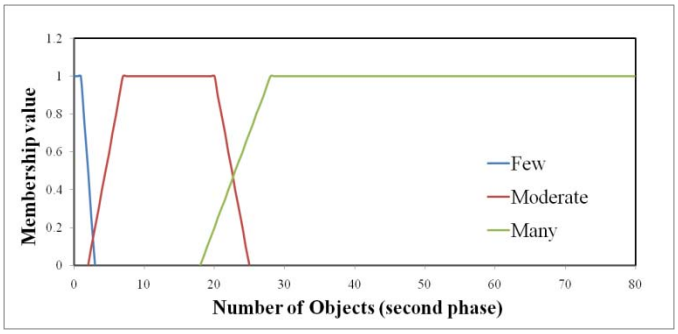

(a)

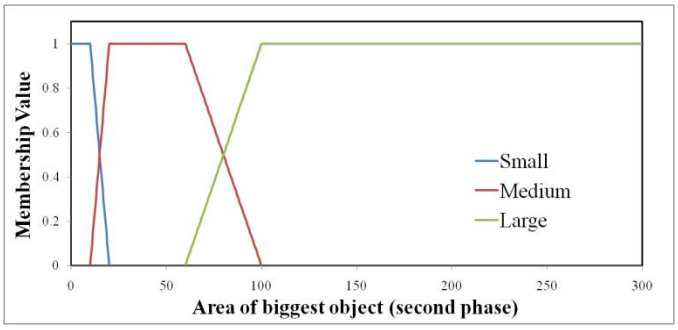

(b)

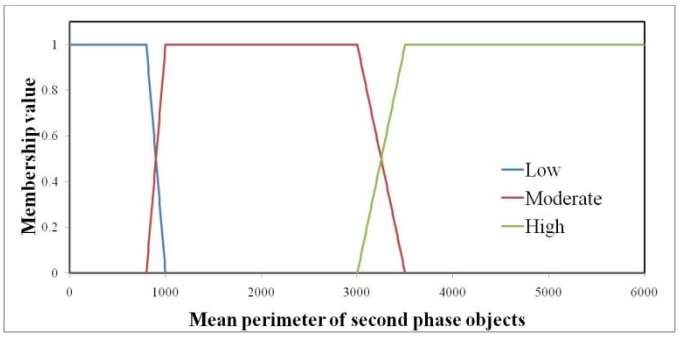

(c)

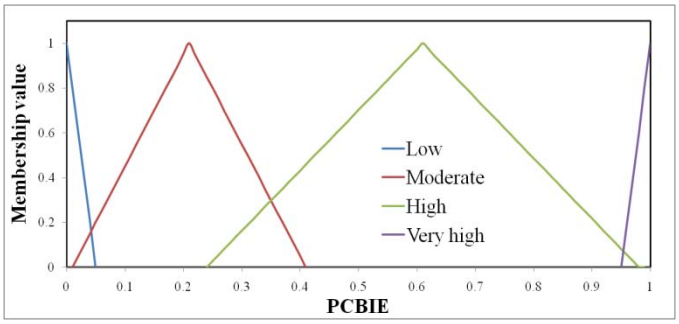

(d)

Fig.14. Membership function for fuzzy inputs a. number of objects, b. area of biggest object, c. mean perimeter of objects and d. PCBIE

The five following steps of a typical fuzzy algorithm were performed [20]:

- Fuzzification of the inputs
- Application of a fuzzy operator "AND by max method" and "OR by min method" among the inputs
- Application of an implication operation (Mamdani min)
- Aggregation of the outputs using the max operator
- Defuzzification of the outputs, using the Center of Area (centroid) method

Figure 15 shows the schematic of fuzzy flow identification system which its inputs are obtained from a simple image processing technique.

Fig.15. Schematic of fuzzy system

Fuzzy Algorithm

In case of our work nine if /then rules were chosen to identify which regime we are in. Table 3 contains the rules we applied to system.

Table3. Rules of fuzzy algorithm

R_1: If *number of objects* is many **then** regime is bubbly; weight of rule = 1

R_2: If *number of objects* is moderate **and** *area of biggest object* is small **and** *mean perimeter* is low **and** *PCBIE* is low **then** regime is bubbly; weight of rule = 1

R_3: If *number of objects* is moderate **and** *PCBIE* is moderate **then** regime is slug; weight of rule = 1

R_4: If *number of objects* is moderate **and** *PCBIE* is high **then** regime is churn; weight of rule = 1

R_5: If *number of objects* is few **and** *PCBIE* is very high **then** regime is annular; weight of rule = 1

R_6: If *area of biggest object* is small **or** *mean perimeter* is low **then** regime is bubbly; weight of rule = 0.5

R_7: If *area of biggest object* is moderate **and** *mean perimeter* is moderate **and** *PCBIE* is moderate **then** regime is slug; weight of rule = 1

R_8: If *area of biggest object* is moderate **and** *mean perimeter* is moderate **and** *PCBIE* is high **then** regime is churn; weight of rule = 1

R_9: If *area of biggest object* is large **and** *mean perimeter* is high **and** *PCBIE* is very high **then** regime is annular; weight of rule = 1

Adaptive Network-based Fuzzy Interface System (ANFIS)

The basic structure of the type of Fuzzy Inference System (FIS) seen thus far is a model that maps input characteristics to input membership functions, input membership function to rules, rules to a set of output characteristics, output characteristics to output membership functions, and the output membership function to a single-valued output or a decision associated with the output. In this method only fixed membership functions were considered that were chosen arbitrarily. Also FIS can be applied to a system whose rules are known or can be known by characteristic of its important variable. But the Neuro-adaptive learning method works similar to neural networks. Neuro-adaptive learning techniques provide a method for the fuzzy modeling procedure to learn information about a data set. Using a given input/output data set, the ANFIS constructs an FIS whose membership function parameters are tuned (adjusted) using either a back-propagation algorithm alone or in combination with a least squares type of method. This adjustment allows fuzzy systems to learn from the data they are modeling. The parameters associated with the membership functions changes through the learning process. The computation of these parameters (or their adjustment) is facilitated by a gradient vector. This gradient vector provides a measure of how well the FIS is modeling the input/output data for a given set of parameters. When the gradient vector is obtained, any of several optimization routines can be applied in order to adjust the parameters to reduce some error measurements. This error measure is usually defined by the sum of the squared difference between actual and desired outputs.

In this work we applied the results of image feature extraction as the input of our ANFIS. A number of input/output data were segregated to check the results of training. FIS was generated using subtractive clustering method. Training of FIS was done by hybrid optimization method and number of epoch was set to 20. Structure of our ANFIS is shown in Fig.16.

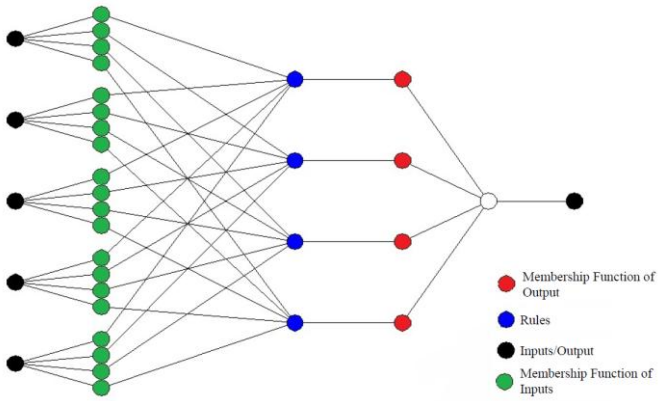

Fig.15. Structure of Adaptive Neuro Fuzzy system

RESULTS AND DISCUSSION

In this part the results of classification with two introduced methods are presented. As we will see two methods can anticipate the flow regime accurately. This section, like previous sections is divided into two parts, one presents the fuzzy modeling results and the other shows ANFIS modelings.

Results of Fuzzy Modeling

Table 4 shows the results of the performed tests. The Mamdani min implication operator has been used for the fuzzy analyses. For each run, the number of objects, area of biggest object, means perimeter of objects, PCBIE and the output of the fuzzy system are reported. The results from the fuzzy algorithm correspond to the prevalent flow (higher membership value) at the given flow output (Fig.13). The results are in good agreement with the visual observation.

However, this simple analysis which is presented in table4 does not allow us to identify the flow pattern transitions. In order to analyze the outputs of the fuzzy system with more accuracy, in Table 5 the values of the membership functions of the different flow regime corresponding to each output of the fuzzy system are provided.

Results of ANFIS Modeling

Figure 17 shows the error of training versus number of epoch. As it is seen after epoch no. 6 the training error remains constant and equal to 0.0109 which is appropriate and acceptable error for training. Fig. 18 demonstrates distribution of testing data and checking data for indexed inputs. It's obvious that these data satisfy testing and checking of trained ANFIS and this method is accurate to identify different flow regimes.

Table4. Output of fuzzy system and defuzzification (all units are pixel)

Case	Visual observation	Number of objects	Area of biggest object $\times 10^4$	Mean perimeter of objects	PCBIE	Flow regime output	Result
1	Bubbly	32	2.5	199	0.01	0.153	Bubbly
2	Bubbly	58	2.6	256	0.03	0.153	Bubbly
3	Bubbly	44	2.1	371	0.03	0.153	Bubbly
4	Bubbly-Slug	21	9.5	601	0.06	0.256	Bubbly
5	Slug	7	21	939	0.17	0.368	Slug
6	Slug	5	39	1270	0.21	0.4	Slug
7	Slug	11	58	1820	0.28	0.422	Slug
8	Slug-Churn	6	86	1603	0.31	0.441	Slug
9	Churn	5	105	1670	0.63	0.6	Churn
10	Churn	3	154	1997	0.74	0.6	Churn
11	Churn	3	182	2218	0.86	0.6	Churn
12	Churn-Annular	3	145	3261	0.92	0.773	Annular
13	Annular	1	191	3919	0.97	0.867	Annular
14	Annular	1	219	4476	0.97	0.867	Annular
15	Annular	1	248	4920	0.98	0.874	Annular
16	Annular	1	231	5049	0.99	0.88	Annular

Table5. Contribution of different flow regime

Case	Visual observation	Bubbly	Slug	Churn	Annular
1	Bubbly	0.97	0	0	0
2	Bubbly	0.97	0	0	0
3	Bubbly	0.97	0	0	0
4	Bubbly-Slug	0.5	0.24	0	0
5	Slug	0.13	0.81	0	0
6	Slug	0	1	0	0
7	Slug	0	0.69	0.08	0
8	Slug-Churn	0	0.49	0.23	0
9	Churn	0	0	0.68	0
10	Churn	0	0	0.29	0
11	Churn	0	0	0.29	0
12	Churn-Annular	0	0	0.11	0.21
13	Annular	0	0	0	0.44
14	Annular	0	0	0	0.44
15	Annular	0	0	0	0.63
16	Annular	0	0	0	0.78

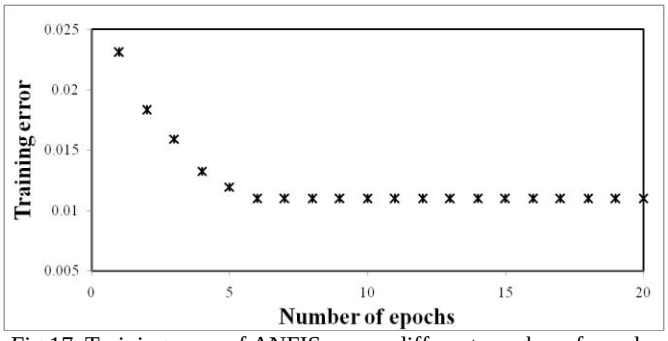

Fig.17. Training error of ANFIS versus different number of epochs

CONCLUSION

Flow regime identifications have been performed thanks to a fuzzy system employing the results from image processing and flow features extraction. Also a new method for image textural features extraction was introduced which are capable to join with Adaptive Neuro Fuzzy Interface System (ANFIS) to classify flow regimes of vertical two phase flow into 4 main regimes. Geometrical parameters of the two-phase flow that depend directly on the flow structures have been used as the inputs of the system. The results are in good agreement with the visual observations and the flow regimes map.

Fuzzy systems and ANFIS are appropriate classifiers of flow regimes. More than indicating which flow regime is prevalent, they give the contribution of each flow regime to the two-phase flow system. This knowledge of the flow can be greatly useful in industrial systems such as petroleum processing or biomedical processing.

ACKNOWLEDGMENT

The authors would like to express their sincere appreciation to Mrs. P.M. Gholampour for her encouragement, support and technical comments on the subject. This research was funded by Iran Supplying Petrochemical Industries Parts, Equipment and Chemical Design Corporation (SPEC) as a joint research project with Sharif University of Technology (project No. KPR-8628077).

(a)

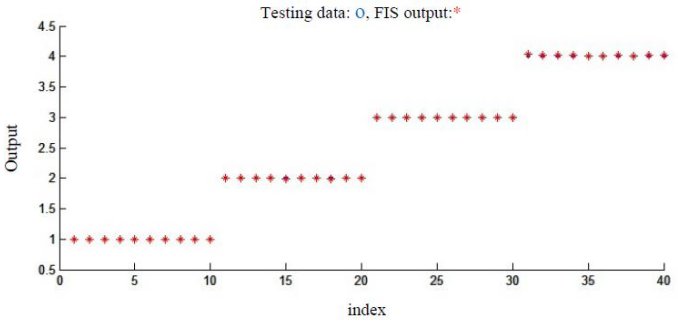

(b)

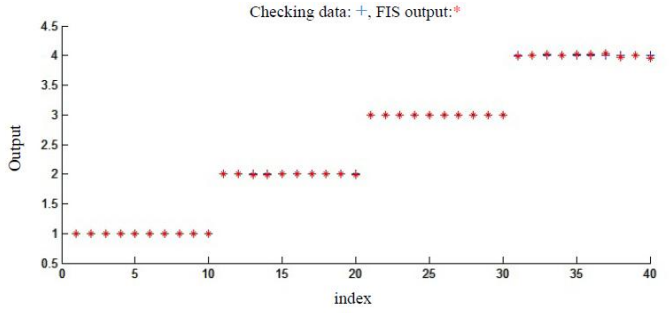

(c)

Fig.18. ANFIS a. training, b. testing and c. checking data versus index of input

REFERENCES

[1] Wallis, G.B., 1969, "One-Dimensional Two-Phase Flow," McGraw-Hill, New York.

[2] Ishii, M., 1975, "Thermo-Fluid Dynamic Theory of Two-Phase Flow," Collectionde la Direction des Etudes et Recherches dı Electricite de France, Eyrolles, Paris.

[3] Taitel, T., Barnea, D., Dukler, A.E., 1980, "Modelling flow pattern transitions for steady upward gas–liquid flow in vertical tubes," AIChE J., Vol. 26, pp. 345–354.

[4] Sun, B., Zhang, H.J., Chen, L., Zhao, Y.X., 2006, "Flow regime identification of gas-liquid two-phase flow based on HHT", Chinese Journal of Chemical Eng., Vol. 14, No. 1, pp. 24-30.

[5] Corre, J.M.L, Aldorwish, Y., Kim, S. and Ishii, M.,1999, "Two-Phase Flow Pattern Identification using a Fuzzy Methodology," Proceeding of International Conference on Information Intelligence and Systems (ICIIS-99), pp. 155.

[6] Mi, Y., Tsoukalas, L.H., Ishii, M., Li, M. and Xiao, Z., 1996, "Hybrid Fuzzy-Neural Flow Identification Technology," IEEE Transactions on Fuzzy Systems, Vol. 2, pp. 1332-1338.

[7] Zhou, Y., Chen, F. and Sun B., 2008, "Identification Method of Gas-Liquid Two-phase Flow Regime Based on Image Multi-feature Fusion and Support Vector Machine," Chinese Journal of Chemical Eng., Vol. 16, No. 6, pp. 832-840.

[8] Shi, L., 2007, "Fuzzy Recognition for Gas-liquid Two-phase Flow Pattern Based on Image Processing," Proceeding of 13rd IEEE International Conference on Control and Automation, pp. 1424-1427.

[9] Sunde, C., Avdic, S. and Pazsit, I., 2005, "Classification of Two-Phase Flow Regimes via Image Analysis and a Neuro-Wavelet Approach," Int. J. of Progress in Nuclear Eng., Vol. 46, No. 3-4, pp. 348-358.

[10] Misawa, M. and Anghaie, S, 1991, "Zero-gravity void fraction and pressure drop in a boiling channel," Proceeding of 27th National Heat Transfer Conference USA, Vol. 87, pp. 226-235.

[11] Gopal, M. and Jepson, W.P., 1997, "Development of digital image analysis techniques for the study of velocity and void profiles in slug flow," Int. J. of Multiphase Flow, Vol. 23, pp. 945-965.

[12] Hesieh, C.C., Wang S.B., Pan, C., 1997, "Dynamic visualization of two-phase flow patterns in a natural circulation loop," Int. J. of Multiphase Flow, Vol. 23, pp. 1147-1170.

[13] Dinh, T.B. and Choi, T.S., 1999, "Application of Image Processing Technique in Air/Water Two Phase Flow," Int. J. Mechanics Research Communications, Vol. 26, No. 4, pp. 463-468.

[14] Shi, L., Zhou, Z. andRen, S., 2004, "Parameter Measurements of Two-phase Bubbly Flow Using Digital Image Processing," Proceedings of the 5th World Congress on Intelligent Control and Automation (IEEE), pp. 3856-3861.

[15] Mayor, T.S., Pinto, A.M.F.R., Campos, A.M.F.R., 2007, "An image analysis technique for the study of gas–liquid slug flow along vertical pipes—associated uncertainty," Int. J. Flow Measurement and Instrumentation, Vol. 18, pp. 139–147.

[16] Wang, H. and Dong, F., 2009, "Image Features Extraction of Gas/liquid Two-Phase Flow in Horizontal Pipe line by GLCM and GLGCM," Proceeding of 9thIEEE International Conference on Electronic Measurement & Instruments, No. 2, pp. 135-139.

[17] Artemiev, V. K. and Kornienko Yu. N., 2002, "Numerical modeling of influence non-monotonic profile of gas content on a distribution of velocity and temperature in a two-phase bubbly flow." Proceeding of 3rd Russian National Conference on Heat Transfer Moscow Russia, Vol. 5, pp. 41–44.

[18] Wang, Z.Y., Jin, N.D., Wang C. and Wang, J.X., 2008, "Temporal and Spatial Evolution Characteristics of Two-phase Flow Pattern Based on Image Texture Analysis," J. Chemical Industrial Eng. (China), Vol. 59, No. 5, pp. 1122-1130.

[19] Haralick, S. K., and Dinstein, I., 1973, "Textural Features for image classification," IEEE Transaction of System, Man and Cybernetics, Vol. SMC-3, No. 6, pp. 610-621.

[20] Tsoukalas, L.H. and Uhrig, R.E., 1997, "Fuzzy and Neural Approaches in Engineering," John Wiley and Sons, New York.